

Magic of Numbers: A Guide for Preliminary Estimation of the Detonation Performance of C–H–N–O Explosives Based on Empirical Formulas

Sergey V. Bondarchuk*

Cite This: *Ind. Eng. Chem. Res.* 2021, 60, 1952–1961

Read Online

ACCESS |

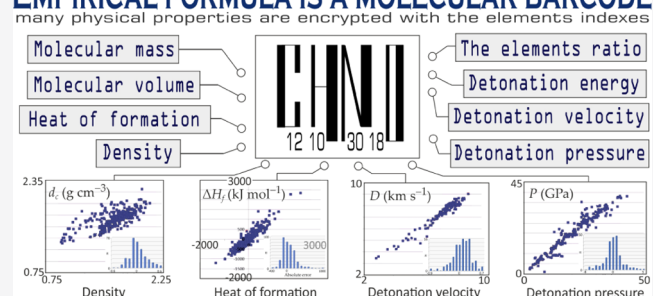
Metrics & More

Article Recommendations

Supporting Information

ABSTRACT: In this paper, we report a comprehensive analytical study of the factors influencing the detonation properties of C–H–N–O explosives. Besides the commonly applied parameters, namely, solid-state enthalpy of formation (ΔH_f) and crystal density (d_c), for which simple zeroth-order additive models based on the atomic increments are developed in this work, we also consider compositional factor being an intrinsic characteristic of each single empirical formula. Using a wide number of reference molecules (320 for ΔH_f and 360 for d_c), we have developed empirical equations, which provide rather good correlation coefficients $R^2 = 0.90$ and 0.80 for ΔH_f and d_c , respectively. Knowing these two equations and empirical formula, one can predict the detonation properties of a C–H–N–O explosive using a pocket calculator. Of course, such an approach, which completely neglects chemical structure, can be applied mainly for structurally similar compounds. However, having significant differences between the predicted detonation properties of two compositions, the account of their exact structures cannot reorder the predicted values. Thus, this paper can be used as a simple guide for molecular engineering and explosive structure enhancement. For this purpose, we provide a list of all compositions with the predicted properties up to $C_{30}H_{30}N_{30}O_{30}$ in the Supporting Information. To demonstrate how it works, we have applied the developed approach along with quantum-chemical calculations to model chemical structures outperforming ϵ -hexanitrohexaazaisowurtzitane (the most powerful explosive) in detonation performance.

EMPIRICAL FORMULA IS A MOLECULAR BARCODE



1. INTRODUCTION

Engineering of new energetic materials is a growing area of research aimed to meet human needs in high-energy-density materials for both civilian and military applications, which must satisfy tight criteria of sensitivity, toxicity, etc.¹ Taking into account risks and costs of such experimental studies, computational supports demonstrate increasing impact in the field. To date, a number of theoretical methods are developed to predict the detonation properties of materials, including heat of detonation; detonation pressure, velocity, and temperature; Gurney energy; and power (strength).² Also, a number of different thermodynamic codes and methods, including various structure–property relationships and neural networks, are developed to perform such calculations;^{3–16} however, currently, the most popular software are EXPLO-5,¹⁷ Cheetah,¹⁸ Lotuses,¹⁹ EMDB,²⁰ etc.

The above-mentioned software calculates chemical equilibrium, the Chapman–Jouguet (CJ) state, iteratively using various equations of state, namely, Becker–Kistiakowsky–Wilson (BKW), Cowan–Fickett, Murnaghan, etc.³ At the same time, a simple empirical scheme was proposed by Kamlet and Jacobs (KJ), which does not assume any iterative procedures

to be applied. As a result, detonation velocity (D) and pressure (P) can be easily obtained using eqs 1 and 2²¹

$$D = A\phi^{1/2}(1 + B\rho_0) \quad (1)$$

$$P = K\rho_0^2\phi \quad (2)$$

where ρ is the density; $A = 1.01$, $B = 1.30$, and $K = 1.558$ are empirical constant, which are applied to best fit the CJ state; and ϕ can be expressed as the follows²¹

$$\phi = N\bar{M}^{1/2}Q^{1/2} \quad (3)$$

where N is the number of moles of gaseous species per gram of the explosive, \bar{M} is the average molecular weight of the gaseous products, and Q is the energy released by the decomposition

Received: November 14, 2020

Revised: January 6, 2021

Accepted: January 7, 2021

Published: January 19, 2021



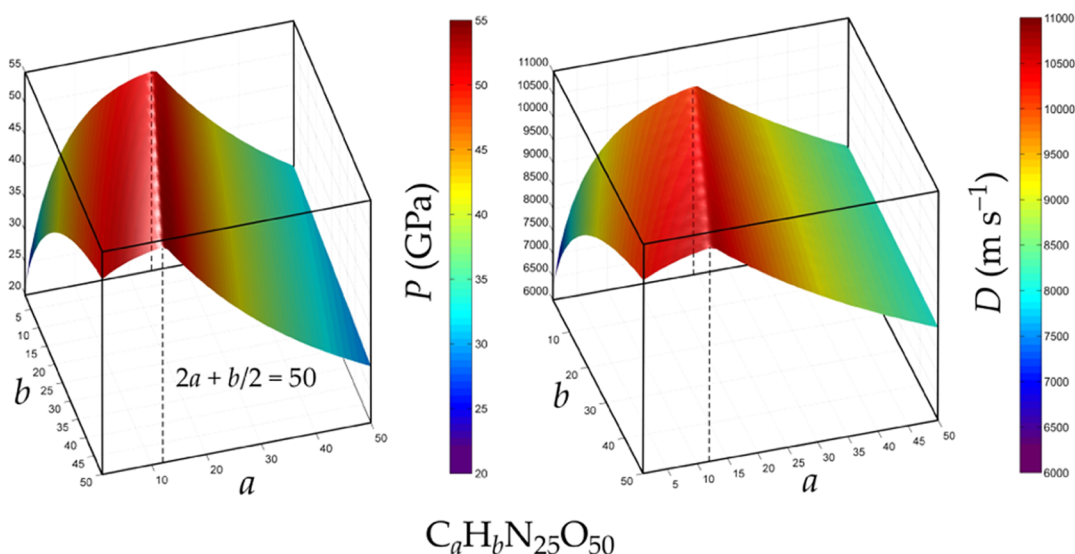


Figure 1. Graphical description of the influence of redox ratio in the molecules of C–H–N–O explosives.

reaction as obtained using the H_2O – CO_2 arbitrary and can be expressed as

$$Q = -\frac{(\sum n\Delta H_f^P) - \Delta H_f^X}{\text{MW}} \quad (4)$$

where ΔH_f^X and ΔH_f^P are the enthalpies of formation of the given explosive X and its detonation products P , scaled by their mole fractions n ; and MW is the molecular weight of X .

In principle, the KJ scheme can be applied beyond the C–H–N–O compositions. In particular, it can be extended to various metal-containing compounds, where metal elements are assumed to form metallic oxides being inert solids that release heat rather than gases.²² On the other hand, if a $\text{C}_a\text{H}_b\text{O}_c\text{N}_d$ composition is considered, then, taking into account the H_2O – CO_2 arbitrary, N , \bar{M} , and Q can be expressed according to their internal oxidation ability (stoichiometric ratio) as follows²³

Ratio I $c \geq 2a + b/2$

$$N = (b + 2c + 2d)/4\text{MW} \quad (5a)$$

$$\bar{M} = 4\text{MW}/(b + 2c + 2d) \quad (6a)$$

$$Q = (28.9b + 94.05a + 239\Delta H_f^0)/\text{MW} \quad (7a)$$

Ratio II $2a + b/2 > c \geq b/2$

In this case, the parameter N is described as in eq 5a.

$$\bar{M} = (56d + 88c - 8b)/(b + 2c + 2d) \quad (6b)$$

$$Q = (28.9b + 94.05(c/2 - b/4) + 239\Delta H_f^0)/\text{MW} \quad (7b)$$

Ratio III $b/2 > c$

$$N = (b + d)/2\text{MW} \quad (5c)$$

$$\bar{M} = (2b + 28d + 32c)/(b + d) \quad (6c)$$

$$Q = (57.8c + 239\Delta H_f^0)/\text{MW} \quad (7c)$$

Recently, we have applied the KJ scheme to predict the D values for seven common explosives (TNT, HNS, RDX, ϵ -CL-20, TKX-50, NTO, and DAAF) and confirmed its reliability since the predicted values appeared to be closest to the experimental ones.²⁴ As it follows from eqs 5a, 5c to 7a–7c, stoichiometry can

significantly affect detonation performance. To demonstrate this, we have performed a series of calculations of D and P values for a variable composition $\text{C}_a\text{H}_b\text{N}_{25}\text{O}_{50}$. Within these calculations, enthalpy was kept constant ($\Delta H_f = 100 \text{ kJ mol}^{-1}$) and density was roughly estimated using the additive model described in Figure S1 in the Supporting Information. It is clearly seen that the line $2a + b/2 = 50$ ($\Omega_{\text{CO}_2} = 0$) corresponds to the maximum performance in both the cases (Figure 1). Thus, empirical formula appears to be a crucial factor determining D and P values.

But what can we say about the influence of density and enthalpy of formation? To demonstrate how the error of prediction of d_c and ΔH_f affects the accuracy of the resulting D and P values, we have performed a series of calculations for RDX (Figure 2). As one can see, within a 1% error for D , the error of

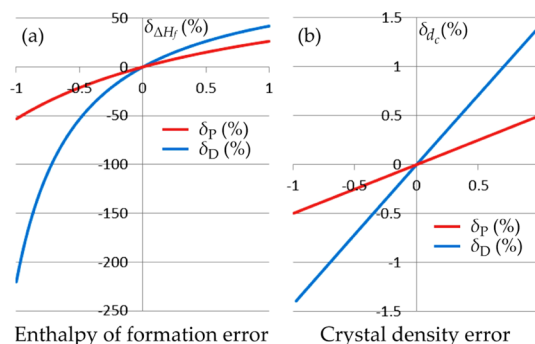


Figure 2. Influence of errors in the prediction of d_c and ΔH_f on the accuracy of the D and P values.

prediction of d_c and ΔH_f can be varied in the ranges of -1.4 – 1.4 and -220.2 – 42.0% , respectively. Similarly, for P , these ranges are -0.5 – 0.5 and -53.0 – 26.4% , respectively. It becomes clear that enthalpy of formation is the least important factor, while stoichiometry and density are much more important. We should stress, however, that the change of a relative error of ΔH_f makes little sense since the origin of the ΔH_f data is a matter of pure convention, in contrast to heats of explosion or detonation energy (Q). For any energetic material whose ΔH_f is sufficiently close to zero, a large relative change in ΔH_f is insignificant as this

represents only a small absolute variation. On the other hand, when applying the KJ scheme, a user does not deal with Q but ΔH_f ; therefore, the influence of the ΔH_f estimation error is of practical interest. Thus, in this paper, we have tried to show how much information one can obtain from a simple chemical composition. This allows us to perform a preliminary crude estimation of a possible structure using a pocket calculator.

2. COMPUTATIONAL DETAILS

All of the calculations of detonation performances were done using our developed code written in the PascalABC.Net programming language. This code can be used in manual and automatic modes. In the latter case, it can predict the d_c , ΔH_f , Ω_{CO_2} , Q , D , and P values within a custom-defined range of $C_xH_yN_zO_w$ compositions and order them according to a custom-defined property. In this work, we provide a list of calculated compositions up to $C_{30}H_{30}N_{30}O_{30}$, which are ranged by the D values (462 241 compositions). Such a number of formulas is determined by the condition (eq 8) that considers only the compositions possessing even sum of the total valences

$$4x + y + 3z + 2w \pmod{2} = 0 \quad (8)$$

The code also has two simplifications: (1) all allotropic compositions have $\Delta H_f = 0$; (2) if $Q < 0$, then $D = P = 0$.

Gibbs tetrahedrons were built using Matlab r2014a. The corresponding input scripts were generated using our other code, which applies eqs 9–11 to set coordinates of a point inside the Gibbs tetrahedron and assigns to it an RGB triplet within the rainbow colormap. The latter corresponds to its calculated property (d_c , ΔH_f , D , or P).

$$x = \frac{az}{200} + \frac{abq(100 - z)}{5000} + \frac{acq(100 - z)}{20\,000} \quad (9)$$

$$y = \frac{az}{200\sqrt{3}} + \frac{\sqrt{3}acq(100 - z)}{20\,000} \quad (10)$$

$$z = d \quad (11)$$

where $a = 50\sqrt{6}$, $b = \text{wt} \%(\text{H})$, $c = \text{wt} \%(\text{C})$, $d = \text{wt} \%(\text{O})$, and $q = -100/(z - 100)$ for $z < 100$.

Quantum-chemical calculations were performed using Gaussian09²⁵ and Materials Studio 2017²⁶ suite of programs for nonperiodic and periodic systems, respectively. Vacuum isolated molecules were optimized using the DFT(ω B97XD)/6-31G(d,p) method,^{27,28} and their Merz–Kollman electrostatic potential fitting partial charges were obtained. Crystal structure predictions were performed with the Polymorph module of the Materials Studio 2017 program suite using ab initio force field COMPASSII (Condensed-phase Optimized Molecular Potentials for Atomistic Simulation Studies).^{29,30} The crystal structure prediction was performed for the following five most frequent space groups: $P2_1/c$ (34.3%), $P\bar{1}$ (25.0%), $C2/c$ (8.3%), $P2_12_12_1$ (7.0%), and $P2_1$ (5.1%).³¹ Then, the lowest-energy structures were applied for crystal density estimation. Lattice energies were calculated in terms of all-electron approximation using pure GGA functional due to Perdew–Burke–Ernzerhof (PBE)³² along with a double-numerical basis set, DNP, as implemented in the DMol³ code.³³ This code allows us to treat both periodic and nonperiodic systems with the same method without use of supercell approximation.

Solid-state enthalpies of formation of model compounds were calculated using eqs 12–14.^{34–36} This method was recently

applied at the B3LYP/6-311++G(2d,2p) level of theory,^{35,36} but this approach is very expensive; thus, we have reparametrized atomic energies for a less expensive ω B97XD/6-31G(d,p) approach.

$$\Delta H_{\text{gas}} = E_{C_xH_yN_zO_w} - (iE_C + jE_H + kE_N + lE_O) \quad (12)$$

$$\Delta H_{\text{sub}} = -E_{\text{latt}} - 2RT = -\frac{E_{\text{solid}}}{Z'} + E_{\text{gas}} - 2RT \quad (13)$$

$$\Delta H_{\text{solid}} = \Delta H_{\text{gas}} - \Delta H_{\text{sub}} \quad (14)$$

where ΔH_{solid} , ΔH_{gas} , and ΔH_{sub} are the solid-state and gas-phase enthalpies of formation and sublimation, respectively, and $E_{C_xH_yN_zO_w}$ and E_X are the ZPE-corrected total energies of the given molecule and the constituting elements in their stationary states (graphite, $1\sum_g^+ \text{H}_2$, $1\sum_g^+ \text{N}_2$, and $3\sum_g^- \text{O}_2$), respectively. At the ω B97XD/6-31G(d,p) level of theory, these values are as follows: $E_C = -38.10444$, $E_H = -0.58064$, $E_N = -54.74804$, and $E_O = -75.12972$ Ha. E_{solid} and E_{gas} are the energies of an asymmetric cell and an isolated molecule, respectively, and Z' is the number of formula units per asymmetric cell.

Thus, the Gaussian09 calculations were performed for calculating: (1) the ΔH_{gas} values from eq 12 and (2) the Merz–Kollman charges needed for Polymorph predictor using the COMPASSII force field. The DMol³ calculations were used to derive sublimation enthalpies from eq 13, after relaxing the lowest-energy crystal structures predicted with Polymorph.

3. RESULTS AND DISCUSSION

3.1. Enthalpy of Formation. First of all, we have tried to quantify enthalpy of formation based on an additive model. Such approaches, which are based on additive schemes of the zeroth (atoms), first (bonds), and second order (groups), were put forward long ago in a seminal paper of Benson and Buss.³⁷ Afterward, such approximations were widely applied but mostly for structural increments (bond and group additivity) for both gas^{38–41} and condensed-phase^{42–47} enthalpies of formation. In our case, we know nothing about the structure (the zeroth-order approximation); therefore, we assume that the structure-dependent term in eq 15 equals zero.

$$\Delta H_f = \frac{x E_C + y E_H + z E_N + w E_O}{\text{structure-independent term}} - \frac{E_{C_xH_yN_zO_w}}{\text{structure-dependent term}} \quad (15)$$

Hence, for an empirical formula, heat of formation can be expressed as a sum of atomic increments multiplied by their indices (eq 16)

$$\Delta H_f = x E_C + y E_H + z E_N + w E_O \quad (16)$$

Such an equation can be solved analytically only when a molecule consists of two elements, for example, a normal hydrocarbon. Using condensed-phase enthalpies of formation for $n\text{-C}_3\text{H}_8$ and $n\text{-C}_{10}\text{H}_{22}$, which equal -119.8 and -301.0 kJ mol⁻¹, respectively,⁴⁸ one can write

$$\begin{vmatrix} 3 & 8 \\ 10 & 22 \end{vmatrix} = \begin{vmatrix} -119.8 \\ -301.0 \end{vmatrix} \quad (17)$$

Solving this system, one obtains $E_C = 16.26$ and $E_H = -21.07$, which means that carbon contributes positively and hydrogen contributes negatively to the ΔH_f values. As a result, any intermediate value is easily obtained, for example, for n -hexane,

Table 1. Values of Slope (*a*) and Intercept (*b*) at Various *n*

entry	<i>n</i> = 1	<i>n</i> = 2	<i>n</i> = 3	<i>n</i> = 4	<i>n</i> = 5	<i>n</i> = 6	<i>n</i> = 7	<i>n</i> = 8	<i>n</i> = 9	<i>n</i> = 10
<i>a</i>	1.1357	0.8529	2.0813	1.0595	5.6788	2.3519	1.3199	0.832	1.3637	0.8409
<i>b</i>	112.24	220.3	243.17	74.857	466.19	223.43	77.867	108.64	198.26	90.717

one can write $(16.26 \times 6) + (-21.07 \times 14) = -197.4 \text{ kJ mol}^{-1}$, while the experimental value is $-198.7 \text{ kJ mol}^{-1}$.⁴⁸

However, when the number of double bonds or degree of unsaturation (eq 18) rises, coefficients E_C and E_H change. Therefore, the best way is to express them via the corresponding values for alkanes ($n = 0$) with different slope (*a*) and intercept (*b*) corrections (Table 1).

$$n = x - y/2 + z/2 + 1 \quad (18)$$

With such correction, the predicted values for 70 hydrocarbons up to $n = 10$ demonstrate a good correlation with experimental ones and provide $R^2 = 0.94$ (Figure 3). The corresponding numerical data along with the chemical names are listed in Table S1 in the Supporting Information.

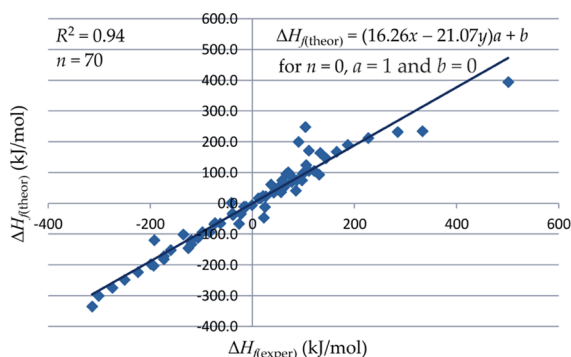


Figure 3. Correlation of the predicted and experimental condensed-phase enthalpies of formation for 70 hydrocarbons.

Unfortunately, for more complex cases, such a simple model cannot be applied since there is no general functional dependence between atomic increments for an arbitrary set of compounds. Therefore, we have used a set of 250 arbitrary C–H–N–O compositions with experimentally known enthalpies of formation and build a system (eq 19)

$$\begin{pmatrix} x_1 E_C & y_1 E_H & z_1 E_N & w_1 E_O \\ x_2 E_C & y_2 E_H & z_2 E_N & w_2 E_O \\ \vdots & \vdots & \vdots & \vdots \\ x_{250} E_C & y_{250} E_H & z_{250} E_N & w_{250} E_O \end{pmatrix} = \begin{pmatrix} \Delta H_f 1 \\ \Delta H_f 2 \\ \vdots \\ \Delta H_f 250 \end{pmatrix} \quad (19)$$

Then, coefficients E_X have been varied with a subsequent least-square fitting of the predicted array of ΔH_f to the corresponding experimental values at each step (Table S2 in the Supporting Information).

As a result, we have obtained a good correlation ($R^2 = 0.90$), which is illustrated in Figure 4. Similar to the previous case, carbon contributes positively ($E_C = 32 \text{ kJ mol}^{-1}$) and hydrogen contributes negatively ($E_H = -26 \text{ kJ mol}^{-1}$). Furthermore, nitrogen also contributes positively ($E_N = 89 \text{ kJ mol}^{-1}$) and oxygen contributes negatively ($E_O = -56 \text{ kJ mol}^{-1}$). Note that the fractional parts of the E_X are omitted, since these do not affect R^2 with such a scattering of ΔH_f values. Thus, now it becomes clear that compounds bearing many carbons and

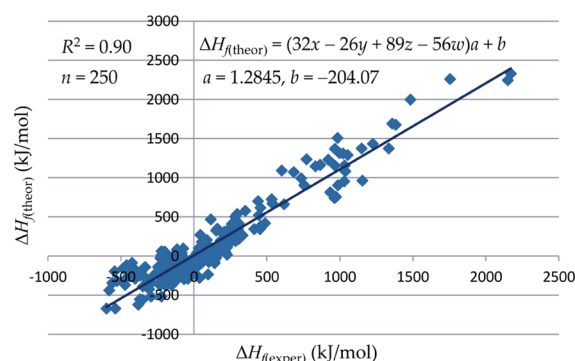


Figure 4. Correlation of the predicted and experimental condensed-phase enthalpies of formation for 250 arbitrary C–H–N–O compositions.

nitrogens should have high ΔH_f values and those bearing many oxygens and hydrogens should have negative ones. For example, 1,1'-azobis(3,5-diazo-1,2,4-triazole) C_4N_{20} has $\Delta H_f = 2150.8$ (2246.8) kJ mol^{-1} ,⁴⁹ while pentaerythritol tetranitrate $C_5H_8N_4O_{12}$ has $\Delta H_f = -538.5$ (-671.6) kJ mol^{-1} .⁴⁸

3.2. Crystal Density. Similar to enthalpy of formation, additive models, which are based on both the higher-^{50–52} and zeroth-order⁵³ approximations, were also applied for density. As in the previous section, we apply the zeroth-order approximation based on pure atomic volumes (Figure 5), which are obtained

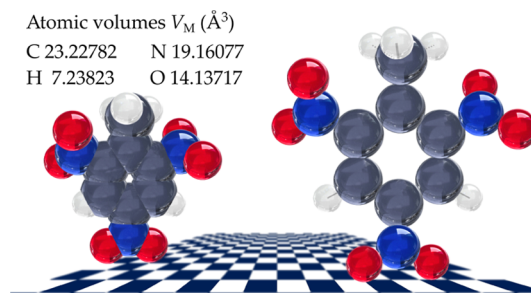


Figure 5. Normal molecule (left) and additive model (right) for 2,4,6-trinitrotoluene as an example.

from the corresponding van der Waals radii.⁵⁴ But unlike a previous work,⁵³ where crystal cell volumes were analyzed to derive average atomic volumes, we have performed an inverse procedure. In the present work, densities are obtained on the basis of a regression equation between the predicted (additive) and real (experimental) crystal densities. Thus, we have used empirical formulas of 360 energetic materials and calculated densities for their additive models (Figure 5). These values correlate well with the corresponding experimental data (Table S3 in the Supporting Information) providing $R^2 = 0.80$; on the basis of this correlation, a regression equation was obtained (eq 20).

$$\rho_{\text{theor}} = \left(\frac{\sum A_r(\text{atoms})}{\sum V_M(\text{atoms})} \right) 2.0755 + 0.3136 \quad (20)$$

The calculated (eq 20) values of d_c against the corresponding experimental densities are illustrated in Figure 6. Despite the d_c

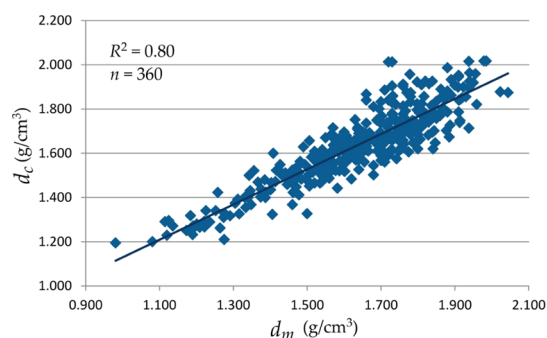


Figure 6. Correlation of the predicted and experimental crystal densities for 360 arbitrary C–H–N–O energetic materials.

values of the most energetic materials vary in a rather narrow range, we have obtained relatively good estimates: $\Delta_{\max} = 0.293$, $\Delta_{\min} = -0.224$, mean = 0, median = 0, mode = 0.036. For absolute values of Δ , the latter three estimates are the following: 0.068, 0.055, and 0.004. Thus, one can conclude that eq 20 is accurate enough to provide a crude estimation of the densities of energetic materials.

3.3. Validation of the Approximation. To check how the described approach can be applied in practice, we have first predicted d_c , ΔH_f , D , and P values for 177 energetic materials of different arbitrary families, which were not used for calibration of eqs 19 and 20 (Table S4 in the Supporting Information). As a result, clear correlations are tracked; however, the correspond-

ing R^2 values are relatively low, being 0.53 for P and 0.41 for D (Figure S2 in the Supporting Information). This means that the presented approach cannot be directly used for comparison of two compositions from structurally very different families.

But what if one compares the predicted D and P within a set of structurally similar compounds? For this purpose, we have chosen four arbitrary families of energetic materials including salts of 1*H*,1'*H*-5,5'-bistetrazole-1,1'-diolate,⁵⁵ 3-(3-dinitromethanide-1*H*-1,2,4-triazol-5-yl)-4-nitraminofurazanate,⁵⁶ di(1*H*-tetrazol-5-yl)methanamine,⁵⁷ and *N,N'*-methylenebis(*N*-(1,2,5-oxadiazol-3-yl)nitramide).⁵⁸ The corresponding numerical data are listed in Table 2. As one can see, the R^2 values are much higher and reach 0.88, which suggests that empirical formula is a crucial criterion, while an exact structure is a minor. Thus, the described approach can be easily applied to search the best composition within a desired structural family or to improve the existing family by variation of cation/anion in energetic salts or by variation of substituents, etc.

Additionally, it is interesting to compare the results of the presented approach with other prediction methods, which take into account exact chemical structures. For this purpose, we have chosen a few papers by Keshavarz et al., where the d_c ,^{59,60} ΔH_f ,^{61,62} D ,⁵³ and P ⁶⁴ values are predicted for a wide number of energetic materials. The results are presented graphically in Figure 7, and the corresponding statistical analysis data are listed in Table 3. The red markers indicate our results, which are obtained without account of chemical structures. We should stress that in some cases, the number of points does not match with the literature data (Table 3). This is because of a restriction of our approach, which considers only C–H–N–O compositions. Also, two points were omitted for the d_c plot, for

Table 2. Validations of the Developed Empirical Models within Each Single Family of Explosives

entry	empirical formula	D (m s ⁻¹)		R^2	P (GPa)		R^2
		literature	this work		literature	this work	
Salts of 1 <i>H</i> ,1' <i>H</i> -5,5'-bistetrazole-1,1'-diolate ⁵⁵							
2	C ₄ H ₅ N ₉ O ₂	8257	7627	0.81	25.9	24.4	0.88
3	C ₄ H ₈ N ₁₀ O ₃	8818	7873		29.9	25.9	
4	C ₄ H ₉ N ₁₁ O ₂	8801	7808		28.9	25.0	
5	C ₄ H ₈ N ₁₀ O ₂	8286	7712		24.9	24.4	
6	C ₅ H ₁₁ N ₁₃ O ₂	8244	7736		23.9	24.3	
7	C ₆ H ₁₂ N ₁₄ O ₃	8138	7644		23.6	23.9	
Salts of 3-(3-dinitromethanide-1 <i>H</i> -1,2,4-triazol-5-yl)-4-nitraminofurazanate ⁵⁶							
4	C ₅ H ₉ N ₁₁ O ₇	8655	8362	0.61	31.3	30.3	0.86
5	C ₅ H ₉ N ₁₁ O ₉	8897	8679		35.8	33.2	
7	C ₇ H ₁₃ N ₁₅ O ₇	7855	8020		22.7	27.2	
8	C ₇ H ₁₅ N ₁₇ O ₇	8385	8088		26.6	27.5	
9	C ₇ H ₁₇ N ₁₉ O ₇	8412	8174		26.5	28.0	
10	C ₇ H ₁₉ N ₂₁ O ₇	8868	8245		30.1	28.4	
Salts of di(1 <i>H</i> -tetrazol-5-yl)methanamine ⁵⁷							
1	C ₃ H ₃ N ₉ O	8226	7811	0.84	27.4	25.8	0.71
2 H ₂ O	C ₃ H ₇ N ₉ O	7371	7695		18.4	24.1	
3 H ₂ O	C ₃ H ₅ N ₉ O ₃	8608	8181		29.6	28.7	
6 H ₂ O	C ₃ H ₁₁ N ₁₁ O ₃	8592	8172		25.0	27.5	
7	C ₃ H ₁₁ N ₁₃ O ₂	8701	8212		27.5	27.6	
Salts of <i>N,N'</i> -methylenebis(<i>N</i> -(1,2,5-oxadiazol-3-yl)nitramide) ⁵⁸							
6 H ₂ O	C ₇ H ₁₂ N ₁₄ O ₁₇	8606	9147	0.60	32.2	37.8	0.76
7 H ₂ O	C ₇ H ₁₄ N ₁₆ O ₁₅	8371	8934		30.3	35.5	
8	C ₉ H ₂₀ N ₂₄ O ₁₄	7996	8585		24.5	31.9	
9	C ₉ H ₁₂ N ₂₄ O ₁₄	8422	8806		29.8	34.3	
10	C ₇ H ₁₀ N ₁₄ O ₁₄	8121	8939		28.0	35.9	

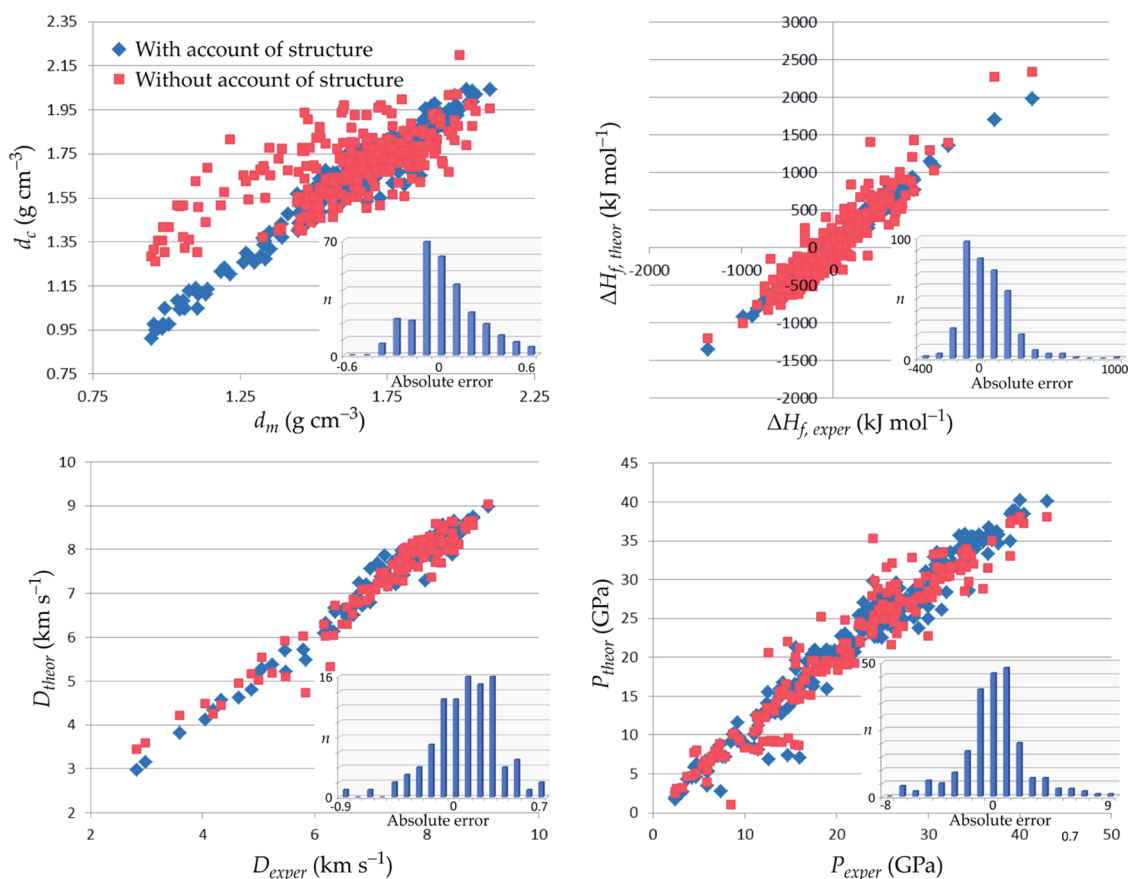


Figure 7. Comparison of effectiveness of the developed approach (red markers) with methods accounting exact chemical structure (blue markers).

Table 3. Statistical Treatment of the Results Described in Figure 7

parameter	<i>n</i>		<i>R</i> ²		RMSE		refs
	literature	this work	literature	this work	literature	this work	
<i>d_c</i>	296	294	0.95	0.47	3.29	10.40	59, 60
ΔH_f	398	377	0.99	0.85	41.31	174.32	61, 62
<i>D</i>	105	105	0.97	0.93	3.11	6.58	63
<i>P</i>	288	222	0.96	0.92	1.81	2.60	64

CH(NO₂)₃ and C(NO₂)₄, since these are reproduced very poorly.

As one can see, the approach presented in this work reproduces experimental results well. Only in the case of crystal density, the value of *R*² is 0.47, while in the rest of cases, *R*² is 0.85, 0.92, and 0.93 (Table 3). At the same time, divergence of the *d_c* prediction results is for a rather narrow range, which can be seen from the corresponding absolute error distribution diagram (Figure 7). Moreover, such a divergence is observed mostly for low-density structures, while the ones possessing *d_c* > 1.5 are predicted better. The most accurate prediction is observed in the range of approximately 1.7–1.9 g cm⁻³, which is characteristic for most energetic materials.

Along with this paper, we provide a supporting information text file containing predicted *d_c*, ΔH_f , Ω_{CO_2} , *Q*, *D*, and *P* values up to C₃₀H₃₀N₃₀O₃₀, which are ranged by the *D* values (462 241 compositions). As one can see, all nitrogen-rich structures are allocated mostly in the top of the list, which means that the method recognizes nitrogen as an increment contributing positively in both enthalpy of formation and density. Thus, we provide a numerical explanation why nitrogen-rich energetic

materials are so effective and possess high enthalpies of formation and high densities.

To provide a simple and convenient presentation of the *d_c*, ΔH_f , *D*, and *P* values as functions of empirical formula, we have built the corresponding Gibbs tetrahedrons (Figure 8). These contain all possible compositions up to C₁₅H₁₅N₁₅O₁₅, and due to a low weight fraction of hydrogen, the points are located mostly near the CNO plane. This allows one to see a clear map of the calculated functions for any single composition. The positions of a few popular explosives are marked inside the tetrahedron. As one can see, some explosives lie almost at the maximum limit of theoretical performance. The highest values appear at the nitrogen corner, which means that the only way to enhance the detonation properties of C–H–N–O explosives is increasing the nitrogen content. It is also seen that ϵ -hexanitrohexaazaisowurtzitane (ϵ -HNIW or CL-20) does not reach the maximum theoretical performance; thus, its structure can be modified to obtain more powerful explosives.

Let us consider what factors make ϵ -HNIW (Figure 9) so powerful. First of all, its high density (2.055 g cm⁻³), which is one of the highest densities among organic molecular crystals.⁶⁵

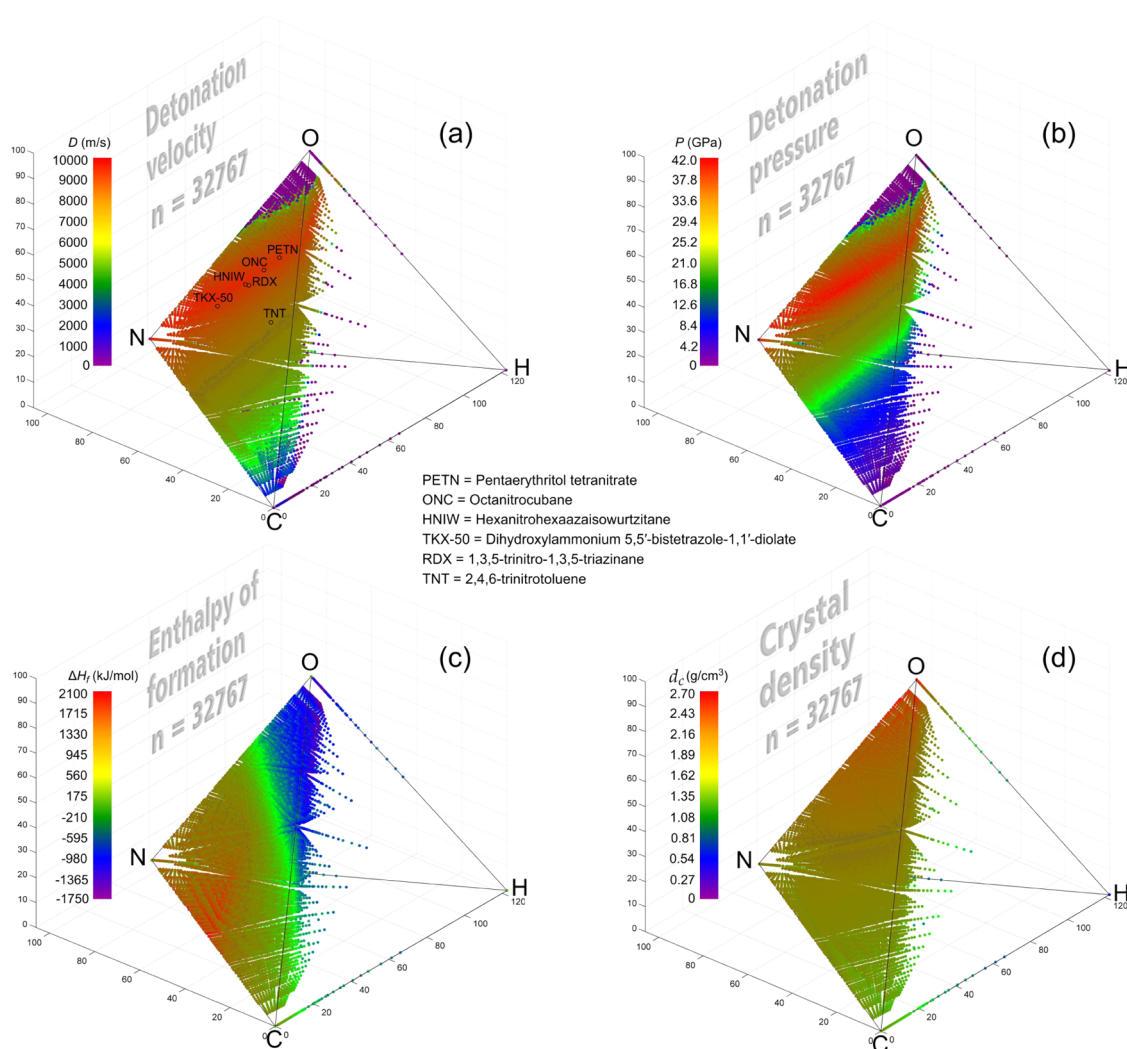


Figure 8. Graphical representation of d_c , ΔH_f , D , and P within the Gibbs tetrahedrons for compositions up to $C_{15}H_{15}N_{15}O_{15}$.

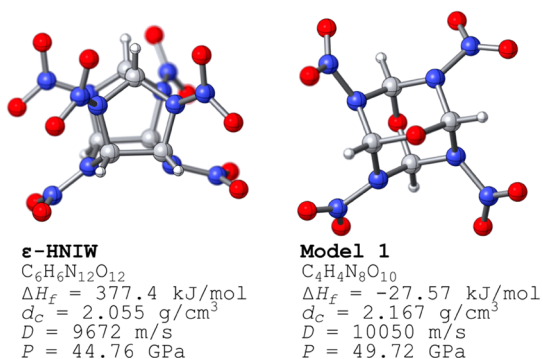


Figure 9. Structure and detonation properties of the reference molecule (ϵ -HNIW) and Model 1.

Despite at least three different values of ΔH_f are reported in the literature as experimental for ϵ -HNIW (454, 415, and 377.4 kJ mol⁻¹),^{66–68} any of them is also high; although, as we have shown in Figure 2, it plays a minor role. In this work, however, we have also calculated solid-state enthalpy of formation of ϵ -HNIW using eqs 12–14 and obtained a value 375.3 kJ mol⁻¹, which is extremely close to the ΔH_f value reported by Simpson et al.⁶⁸ It is interesting that the empirical value of ΔH_f for $C_6H_6N_{12}O_{12}$ obtained using additive scheme is 350.8 kJ mol⁻¹

(see the Supporting Information). The combination of high d_c and ΔH_f , along with its compositional criterion, makes ϵ -HNIW the most powerful explosive known.^{69–71} We should stress that there are a number of different data on its D and P ,^{72–74} therefore, in this work, we trust only own results obtained in terms of the KJ scheme (Figure 9).

Analyzing the structures of three the most dense C–N–H–O compounds, namely, ϵ -HNIW, heptanitrocubane (2.024 g cm⁻³),⁷⁵ and tetranitroglycoluril (2.04 g cm⁻³),⁷⁶ one can deduce that a cage structure, which includes both the N–NO₂ moieties and hydrogen atoms should yield high density and ΔH_f . Thus, using our list of compositions in the Supporting Information, we have found that $C_4H_4N_8O_{10}$ (no. 21750 in the rating) is superior to ϵ -HNIW ($C_6H_6N_{12}O_{12}$, no. 56073 in the rating) and such a composition can be representative of a structural hybrid of ϵ -HNIW and tetranitroglycoluril (Figure 9, Model 1). Thus, we have calculated densities and enthalpies of formation of Models 1–5 as well as ϵ -HNIW for comparison (Figure S3 and Table S5 in the Supporting Information).

As one can see, all of the models demonstrate higher densities than ϵ -HNIW. Moreover, its calculated density (1.982 g cm⁻³) is lower than the corresponding experimental value. Therefore, the experimental densities of Models 1–5 may be expected even higher. Thus, our calculations revealed that all of the proposed structures, except of Model 2, are more powerful explosives than

ε -HNIW (Figure 9 and S3 in the Supporting Information). Despite the lower or even negative (Model 1) enthalpies of formation, this is achieved due to other major criteria, namely, density and composition. As it follows from Figure S3, the information obtained from empirical formula is absolutely enough for a correct prediction of detonation properties of ε -HNIW and Models 1–5, and this is an example of how the results of this work can be used in practice.

4. CONCLUSIONS

In summary, we have shown in this paper that detonation performance of explosives is largely predetermined by their empirical formula and the structural influence is minor. This means that compositional influence can be estimated a priori, which was done in the present work for a wide set of compositions up to $C_{30}H_{30}N_{30}O_{30}$. Moreover, the developed empirical regression equations for d_c and ΔH_f allow one to repeat this calculation for any other $C_xH_yN_zO_w$ composition with a pocket calculator. Though we considered only C–H–N–O compositions, such an approach can be extended to a larger set of elements (halogens, metals, etc.), for which the H_2O – CO_2 arbitrary decompositions products are known.

Of course, the developed approach cannot be directly applied for the prediction of the detonation properties for an arbitrary composition, since in this case, an account of exact structure is required;^{77–79} the same situation is for any other quantitative structure–property relationship, like prediction of flammability limit temperature⁸⁰ or impact sensitivity.⁸¹ On the other hand, our approach can be effectively used to design new high-performance explosives or modify existing ones. In the case of big difference in the predicted properties for two C–H–N–O compositions, structure cannot reorder them; therefore, one can easily estimate how much a proposed structure should be different from a reference molecule, say ε -HNIW ($C_6H_6N_{12}O_{12}$). This allowed us to propose a very effective energetic material, which is expected to have detonation properties superior to that of ε -HNIW.

Certainly, besides chemical structure, the other fine effects can influence the detonation properties due to the influence on the density, like in the case of hepta- and octanitrocubanes, where the presence of the hydrogen atoms leads to a higher density of the heptanitro derivative.⁷⁵ Therefore, high-level quantum-chemical calculations are always required when predicting the detonation properties of any particular structure, but with the present work, such studies can be performed more purposefully.

■ ASSOCIATED CONTENT

Supporting Information

The Supporting Information is available free of charge at <https://pubs.acs.org/doi/10.1021/acs.iecr.0c05607>.

Empirical scheme for crystal density estimation, condensed-phase enthalpies of formation, densities, general validations of the developed empirical models, and optimized structures of modeled compounds (PDF)

(ZIP)

■ AUTHOR INFORMATION

Corresponding Author

Sergey V. Bondarchuk – Department of Chemistry and Nanomaterials Science, Bogdan Khmelnytsky Cherkasy National University, 18031 Cherkasy, Ukraine; orcid.org/

0000-0002-3545-0736; Phone: (+3) 80472 37-65-76;

Email: bondchem@cdu.edu.ua; Fax: (+3) 80472 37-21-42

Complete contact information is available at:
<https://pubs.acs.org/10.1021/acs.iecr.0c05607>

Notes

The author declares no competing financial interest.

■ ACKNOWLEDGMENTS

This work was supported by the Ministry of Education and Science of Ukraine, Research Fund (grant no. 0117U003908).

■ REFERENCES

- (1) Keshavarz, M. H.; Klapötke, T. M. *The Properties of Energetic Materials Sensitivity, Physical and Thermodynamic Properties*; De Gruyter: Berlin, 2018; pp 1–34.
- (2) Keshavarz, M. H.; Klapötke, T. M. *Energetic Compounds Methods for Prediction of their Performance*; De Gruyter: Berlin, 2017; pp 37–82.
- (3) Koch, E. C.; Weiser, V.; Webb, R. *Review on Thermochemical Codes*; NATO MSIAC Report O-138; Brussels, Belgium, February, 2011.
- (4) *SPEED 3.2.1*, NUMERICS Software GmbH, Petershausen, Germany, 2019.
- (5) Keshavarz, M. H.; Zamani, A. A Simple and Reliable Method for Predicting the Detonation Velocity of CHNOFCl and Aluminized Explosives. *Cent. Eur. J. Energ. Mater.* **2015**, *12*, 13–33.
- (6) Cooper, D. *PROPEP 3*, Software Programme by 2012 MS Windows 7 for Free Distribution Expanded Data File (pepcoded.Daf) for the PROPEP Program, 2012.
- (7) Alibakhshi, A.; Mirshahvalad, H.; Alibakhshi, S. A Modified Group Contribution Method for Accurate Prediction of Flash Points of Pure Organic Compounds. *Ind. Eng. Chem. Res.* **2015**, *54*, 11230–11235.
- (8) Chandrasekaran, N.; Oommen, C.; Sanal Kumar, V. R.; Lukin, A. N.; Abrukov, V. S.; Anufrieva, D. A. Prediction of Detonation Velocity and N-O Composition of High Energy C-H-N-O Explosives by Means of Artificial Neural Networks. *Propellants, Explos., Pyrotech.* **2019**, *44*, 579–587.
- (9) Elton, D. C.; Boukouvalas, Z.; Butrico, M. S.; Fuge, M. D.; Chung, P. W. Applying Machine Learning Techniques to Predict the Properties of Energetic Materials. *Sci. Rep.* **2018**, *8*, No. 9059.
- (10) Jensen, T. L.; Moxnes, J. F.; Unneberg, E.; Christensen, D. Models for Predicting Impact Sensitivity of Energetic Materials based on the Trigger Linkage Hypothesis and Arrhenius Kinetics. *J. Mol. Model.* **2020**, *26*, No. 65.
- (11) Guo, D.; Zybin, S. V.; An, Q.; Goddard, W. A., III; Huang, F. Prediction of the Chapman-Jouguet Chemical Equilibrium State in a Detonation Wave from First Principles Based Reactive Molecular Dynamics. *Phys. Chem. Chem. Phys.* **2016**, *18*, 2015–2022.
- (12) Li, X.-H.; Zhao, F.; Qin, J.-C.; Pei, H.-B. A New Method for Predicting the Detonation Velocity of Explosives with Micrometer Aluminum Powders. *Propellants, Explos., Pyrotech.* **2018**, *43*, 333–341.
- (13) Stine, J. R. On Predicting Properties of Explosives – Detonation Velocity. *J. Energ. Mater.* **1990**, *8*, 41–73.
- (14) Willer, R. L. Calculation of the Density and Detonation Properties of C, H, N, O and F Compounds: Use in the Design and Synthesis of New Energetic Materials. *J. Mex. Chem. Soc.* **2009**, *53*, 108–119.
- (15) Fayet, G.; Rotureau, P.; Joubert, L.; Adamo, C. Predicting Explosibility Properties of Chemicals from Quantitative Structure-Property Relationships. *Process Saf. Prog.* **2010**, *29*, 359–371.
- (16) Kang, P.; Liu, Z.; Abou-Rachid, H.; Guo, H. Machine-learning Assisted Screening of Energetic Materials. *J. Phys. Chem. A* **2020**, *124*, 5341–5351.
- (17) Súčeska, M. Calculation of Detonation Parameters by EXPLOS Computer Program. *Mater. Sci. Forum* **2004**, *465–466*, 325–330.

- (18) Sorin, B.; Laurence, E. F.; Kurt, R. G.; Howard, W. M.; Feng, W. K.; Souers, P. C.; Vitello, P. A. *Cheetah 7.0, rev2280*, Lawrence Livermore National Laboratory, 2012.
- (19) Muthurajan, H.; Sivabalan, R.; Talawar, M. B.; Asthana, S. N. Computer Simulation for Prediction of Performance and Thermodynamic Parameters of High Energy Materials. *J. Hazard. Mater.* **2004**, *112*, 17–33.
- (20) Keshavarz, M. H.; Klapötke, T. M.; Súčeska, M. Energetic Materials Designing Bench (EMDB), Version 1.0. *Propellants, Explos., Pyrotech.* **2017**, *42*, 854–856.
- (21) Kamlet, M. J.; Jacobs, S. J. Chemistry of Detonations. I. A Simple Method for Calculating Detonation Properties of C-H-N-O Explosives. *J. Chem. Phys.* **1968**, *48*, 23–35.
- (22) Wang, Y.; Zhang, J.; Su, H.; Li, S.; Zhang, S.; Pang, S. A Simple Method for the Prediction of the Detonation Performances of Metal-Containing Explosives. *J. Phys. Chem. A* **2014**, *118*, 4575–4581.
- (23) Qiu, L.; Gong, X.; Wang, G.; Zheng, J.; Xiao, H. Looking for High Energy Density Compounds among 1,3-Bishomopentaprismane Derivatives with CN, NC, and ONO₂ Groups. *J. Phys. Chem. A* **2009**, *113*, 2607–2614.
- (24) Bondarchuk, S. V.; Yefimenko, N. A. An Algorithm for Evaluation of Potential Hazards in Research and Development of New Energetic Materials in Terms of their Detonation and Ballistic Profiles. *Propellants, Explos., Pyrotech.* **2018**, *43*, 818–824.
- (25) Frisch, M. J.; Trucks, G. W.; Schlegel, H. B.; Scuseria, G. E.; Robb, M. A.; Cheeseman, J. R.; Scalmani, G.; Barone, V.; Mennucci, B.; Petersson, G. A. et al. *Gaussian 09*, Revision A.02; Gaussian, Inc.: Wallingford, CT, 2009.
- (26) *Materials Studio 2017*; Dassault Systèmes BIOVIA: San Diego, CA, 2016.
- (27) Chai, J.-D.; Head-Gordon, M. Long-range corrected hybrid density functionals with damped atom–atom dispersion corrections. *Phys. Chem. Chem. Phys.* **2008**, *10*, 6615–6620.
- (28) Hehre, W. J.; Radom, L.; Schleyer, P. v. R.; Pople, J. A. *Ab Initio Molecular Orbital Theory*; Wiley: New York, 1986.
- (29) Sun, H. COMPASS: An ab Initio Forcefield Optimized for Condensed-Phase Applications – Overview with Details on Alkane and Benzene Compounds. *J. Phys. Chem. B* **1998**, *102*, 7338–7364.
- (30) Sun, H.; Jin, Z.; Yang, C.; Akkermans, R. L. C.; Robertson, S. H.; Spenley, N. A.; Miller, S.; Todd, S. M. COMPASS II: Extended Coverage for Polymer and Drug-Like Molecule Databases. *J. Mol. Model.* **2016**, *22*, No. 47.
- (31) CSD Space Group Statistics – Space Group Number Ordering 2020 <https://www.ccdc.cam.ac.uk/> (accessed Nov 4, 2020).
- (32) Perdew, J. P.; Burke, K.; Ernzerhof, M. Generalized Gradient Approximation Made Simple. *Phys. Rev. Lett.* **1996**, *77*, 3865–3868.
- (33) Delley, B. From Molecules to Solids with the DMol³ Approach. *J. Chem. Phys.* **2000**, *113*, 7756–7764.
- (34) Byrd, E. F. C.; Rice, B. M. Improved Prediction of Heats of Formation of Energetic Materials using Quantum Mechanical Calculations. *J. Phys. Chem. A* **2006**, *110*, 1005–1013.
- (35) Bondarchuk, S. V. Modeling of Explosives: 1,4,2,3,5,6-Dioxatetrazinane as a New Green Energetic Material with Enhanced Performance. *J. Phys. Chem. Solids* **2020**, *142*, No. 109458.
- (36) Bondarchuk, S. V. Theoretical Evaluation of Hexazinane as a Basic Component of Nitrogen-Rich Energetic Onium Salts. *Mol. Syst. Des. Eng.* **2020**, *5*, 1003–1011.
- (37) Benson, S. W.; Buss, J. H. Additivity Rules for the Estimation of Molecular Properties. Thermodynamic Properties. *J. Chem. Phys.* **1958**, *29*, 546–572.
- (38) Cohen, N.; Benson, S. W. Estimation of Heats of Formation of Organic Compounds by Additivity Methods. *Chem. Rev.* **1993**, *93*, 2419–2438.
- (39) Paraskevas, P. D.; Sabbe, M. K.; Reyniers, M.-F.; Papayannakos, N.; Marin, G. B. Group Additive Values for the Gas-Phase Standard Enthalpy of Formation, Entropy and Heat Capacity of Oxygenates. *Chem. - Eur. J.* **2013**, *19*, 16431–16452.
- (40) Shaikhislamov, D. S.; Talipov, M. R.; Khursan, S. L. Quantum-Chemical and Group-Additive Calculations of the Enthalpies of Formation of Hydroxylamines and Oximes. *Russ. J. Phys. Chem. A* **2007**, *81*, 235–240.
- (41) Sabbe, M. K.; Saeys, M.; Reyniers, M. F.; Marin, G. B.; Van Speybroeck, V.; Waroquier, M. Group Additive Values for the Gas Phase Standard Enthalpy of Formation of Hydrocarbons and Hydrocarbon Radicals. *J. Phys. Chem. A* **2005**, *109*, 7466–7480.
- (42) Domalski, E. S.; Hearing, E. D. Estimation of the Thermodynamic Properties of C-H-N-O-S-Halogen Compounds at 298.15 K. *J. Phys. Chem. Ref. Data* **1993**, *22*, 805–1159.
- (43) Salmon, A.; Dalmazzone, D. Prediction of Enthalpy of Formation in the Solid State (at 298.15K) using Second-Order Group Contributions. Part 1. Carbon-Hydrogen and Carbon-Hydrogen-Oxygen Compounds. *J. Phys. Chem. Ref. Data* **2006**, *35*, 1443–1457.
- (44) Salmon, A.; Dalmazzone, D. Prediction of Enthalpy of Formation in the Solid State (at 298.15K) Using Second-Order Group Contributions—Part 2: Carbon-Hydrogen, Carbon-Hydrogen-Oxygen, and Carbon-Hydrogen-Nitrogen-Oxygen Compounds. *J. Phys. Chem. Ref. Data* **2007**, *36*, 19–58.
- (45) Liebman, J. F.; Greenberg, A. Estimation by Bond-Additivity Schemes of the Relative Thermodynamic Stabilities of Three-Membered-Ring Systems and their Open Dipolar Forms. *J. Org. Chem.* **1974**, *39*, 123–130.
- (46) Smith, D. W. Additive Bond Energy Scheme for the Calculation of Enthalpies of Formation and Bond Dissociation Energies for Alkyl Radicals. *J. Chem. Soc., Faraday Trans.* **1996**, *92*, 4415–4417.
- (47) Mathieu, D. Atom Pair Contribution Method: Fast and General Procedure To Predict Molecular Formation Enthalpies. *J. Chem. Inf. Model.* **2018**, *58*, 12–26.
- (48) NIST Chemistry WebBook <https://webbook.nist.gov/chemistry/> (accessed Nov 4, 2020).
- (49) Li, Y.; Wang, B.; Chang, P.; Hu, J.; Chen, T.; Wang, Y.; Wang, B. Novel catenated N₆ energetic compounds based on substituted 1,2,4-triazoles: synthesis, structures and properties. *RSC Adv.* **2018**, *8*, 13755–13763.
- (50) Mathieu, D.; Bouteloup, R. Reliable and Versatile Model for the Density of Liquids Based on Additive Volume Increments. *Ind. Eng. Chem. Res.* **2016**, *55*, 12970–12980.
- (51) Ye, C.; Shreeve, J. M. Rapid and Accurate Estimation of Densities of Room-Temperature Ionic Liquids and Salts. *J. Phys. Chem. A* **2007**, *111*, 1456–1461.
- (52) Beaucamp, S.; Mathieu, D.; Agafonov, V. Optimal Partitioning of Molecular Properties into Additive Contributions: the Case of Crystal Volumes. *Acta Crystallogr., Sect. B: Struct. Sci.* **2007**, *63*, 277–284.
- (53) Hofmann, D. W. M. Fast Estimation of Crystal Densities. *Acta Cryst.* **2002**, *B58*, 489–493.
- (54) Interactive Periodic Table with Properties of the Elements <https://www.webelements.com/> (accessed Nov 4, 2020).
- (55) Shang, Y.; Jin, B.; Peng, R.; Guo, Z.; Liu, Q.; Zhao, J.; Zhang, Q. Nitrogen-Rich Energetic Salts of 1H,1'H-5,5'-Bistetrazole-1,1'-diolate: Synthesis, Characterization, and Thermal Behaviors. *RSC Adv.* **2016**, *6*, 48590–48598.
- (56) Tang, Y.; He, C.; Imler, G. H.; Parrish, D. A.; Shreeve, J. M. Energetic Furazan-Triazole Hybrid with Dinitromethyl and Nitramino Groups: Decreasing Sensitivity via the Formation of a Planar Anion. *Dalton Trans.* **2019**, *48*, 7677–7684.
- (57) Zhao, G.; He, C.; Gao, H.; Imler, G. H.; Parrish, D. A.; Shreeve, J. M. Improving the Density and Properties of Nitrogen-rich Scaffolds by the Introduction of a C–NO₂ Group. *New J. Chem.* **2018**, *42*, 16162–16166.
- (58) Yu, Q.; Imler, G. H.; Parrish, D. A.; Shreeve, J. M. N,N'-Methylenebis(N-(1,2,5-Oxadiazol-3-yl)nitramide) Derivatives as Metal-Free Green Primary Explosives. *Dalton Trans.* **2018**, *47*, 12661–12666.
- (59) Keshavarz, M. H.; Soury, H.; Motamedoshariati, H.; Dashtizadeh, A. Improved Method for Prediction of the Density of Energetic Compounds using their Molecular Structure. *Struct. Chem.* **2015**, *26*, 455–466.
- (60) Keshavarz, M.; Ebadpour, R.; Jafari, M. A Simple Approach for Predicting the Density of High Nitrogen Organic Compounds as

Materials for Providing Clean Products and Enormous Energy Release. *Cent. Eur. J. Energ. Mater.* **2020**, *17*, 296–317.

(61) Nazari, B.; Keshavarz, M. H.; Hamadian, M.; Mosavi, S.; Ghaedsharafi, A. R.; Pouretedal, H. R. Reliable Prediction of the Condensed (Solid or Liquid) Phase Enthalpy of Formation of Organic Energetic Materials at 298 K through their Molecular Structures. *Fluid Phase Equilib.* **2016**, *408*, 248–258.

(62) Jafari, M.; Keshavarz, M. H.; Noorbala, M. R.; Kamalvand, M. A. Reliable Method for Prediction of the Condensed Phase Enthalpy of Formation of High Nitrogen Content Materials through their Gas-Phase Information. *ChemistrySelect* **2016**, *1*, 5286–5296.

(63) Keshavarz, M. H.; Kamalvand, M.; Jafari, M.; Zamani, A. An Improved Simple Method for the Calculation of the Detonation Performance of CHNOFCl, Aluminized, and Ammonium Nitrate Explosives. *Cent. Eur. J. Energ. Mater.* **2016**, *13*, 381–396.

(64) Jafari, M.; Keshavarz, M. H. A Simple Method for Calculating the Detonation Pressure of Ideal and Non-Ideal Explosives Containing Aluminum and Ammonium Nitrate. *Cent. Eur. J. Energ. Mater.* **2017**, *14*, 966–983.

(65) Xinqi, Z.; Nicheng, S. Crystal and Molecular Structures of *e*-HNIW. *Chin. Sci. Bull.* **1996**, *41*, 574–576.

(66) Nair, U. R.; Sivabalan, R.; Gore, G. M.; Geetha, M.; Asthana, S. N.; Singh, H. Hexanitrohexaazaisowurtzitane (HNIW) and HNIW-Based Formulations. *Combust., Explos. Shock Waves* **2005**, *41*, 121–132.

(67) Lobbecke, S.; Bohn, M. A.; Pfeil, A.; Krause, H. In *Thermal Behaviour and Stability of HNIW (CL-20)*, Proceedings of the 29th International Annual Conference on ICT; Karlsruhe, 1998; p 145.

(68) Simpson, R. L.; Urtiew, P. A.; Ornellas, D. L.; Moody, G. L.; Scribner, K. J.; Hoffman, D. M. CL-20 Performance Exceeds That of HMX and its Sensitivity is Moderate. *Propellants, Explos., Pyrotech.* **1997**, *22*, 249–255.

(69) Geetha, M.; Nair, U. R.; Sarwade, D. B.; Gore, G. M.; Asthana, S. N.; Singh, H. Studies on CL-20: The Most Powerful High Energy Material. *J. Therm. Anal. Calorim.* **2003**, *73*, 913–922.

(70) Nair, U. R.; Gore, G. M.; Sivabalan, R.; Satpute, R. S.; Asthan, S. N.; Singh, H. Studies on Polymer Coated CL-20-The Most Powerful Explosive. *J. Polym. Mater.* **2004**, *21*, 377–382.

(71) Braithwaite, P. C.; Hatch, R. L.; Lee, K.; Wardle, R. B. In *Development of High Performance HNIW Explosive Formulations*, Proceedings of the 29th International Annual Conference on ICT, Karlsruhe, 1998; p 1.

(72) Krause, H. H. New Energetic Materials. In *Energetic Materials: Particle Processing and Characterization*; Teipel, U., Ed.; WILEY-VCH: Weinheim, 2005; pp 1–25.

(73) Ghule, V. D.; Jadhav, P. M.; Patil, R. S.; Radhakrishnan, S.; Soman, T. Quantum-Chemical Studies on Hexaazaisowurtzitanes. *J. Phys. Chem. A* **2010**, *114*, 498–503.

(74) Tang, Y.; Mitchell, L. A.; Imler, G. H.; Parrish, D. A.; Shreeve, J. M. Ammonia Oxide as a Building Block for High-Performance and Insensitive Energetic Materials. *Angew. Chem., Int. Ed.* **2017**, *56*, 5894–5898.

(75) Zhang, M.-X.; Eaton, P. E.; Gilardi, R. Hepta- and Octanitrocubanes. *Angew. Chem., Int. Ed.* **2000**, *39*, 401–404.

(76) Sherrill, W. M.; Johnson, E. C. Preparation of Tetranitroglycoluril. U.S. Patent US9,695,1772017.

(77) Mathieu, D. Sensitivity of Energetic Materials: Theoretical Relationships to Detonation Performance and Molecular Structure. *Ind. Eng. Chem. Res.* **2017**, *56*, 8191–8201.

(78) Mathieu, D. Simple Alternative to Neural Networks for Predicting Sublimation Enthalpies from Fragment Contributions. *Ind. Eng. Chem. Res.* **2012**, *51*, 2814–2819.

(79) Mathieu, D. Accurate or Fast Prediction of Solid-State Formation Enthalpies Using Standard Sublimation Enthalpies Derived From Geometrical Fragments. *Ind. Eng. Chem. Res.* **2018**, *57*, 13856–13865.

(80) Mathieu, D. Physics-Based Modeling of Chemical Hazards in a Regulatory Framework: Comparison with Quantitative Structure–Property Relationship (QSPR) Methods for Impact Sensitivities. *Ind. Eng. Chem. Res.* **2016**, *55*, 7569–7577.

(81) Mathieu, D. Power Law Expressions for Predicting Lower and Upper Flammability Limit Temperatures. *Ind. Eng. Chem. Res.* **2013**, *52*, 9317–9322.